



1 **Alteration of nitrous oxide emissions from floodplain soils by** 2 **aggregate size, litter accumulation and plant soil interactions**

3 Martin Ley^{1,2}, Moritz F. Lehmann², Pascal A. Niklaus³, and Jörg Luster¹

4 ¹Swiss Federal Institute for Forest, Snow and Landscape Research WSL, Zürcherstrasse 111, 8903 Birmensdorf,
5 Switzerland

6 ²Department of Environmental Sciences, University of Basel, Bernoullistrasse 30, 4056 Basel, Switzerland

7 ³Department of Evolutionary Biology and Environmental Studies, University of Zürich, Winterthurerstrasse 190,
8 8057 Zurich, Switzerland

9 *Correspondence to:* Martin Ley (martin.ley@wsl.ch)

10 **Abstract.** Semi-terrestrial soils such as floodplain soils are considered potential hotspots of nitrous oxide (N₂O)
11 emissions. Microhabitats in the soil, such as within and outside of aggregates, in the detritosphere, and/or in the
12 rhizosphere, are considered to promote and preserve specific redox conditions. Yet, our understanding of the
13 relative effects of such microhabitats and their interactions on N₂O production and consumption in soils is still
14 incomplete. Therefore, we assessed the effect of aggregate size, buried organic matter, and rhizosphere processes
15 on the occurrence of enhanced N₂O emissions under simulated flooding/drying conditions in a mesocosm
16 experiment. We used two model soils with equivalent structure and texture, comprising macroaggregates (4000–
17 250 μm) or microaggregates (< 250 μm) from a N-rich floodplain soil. These model soils were either planted
18 with basket willow (*Salix viminalis* L.), mixed with leaf litter, or left unamended. After 48 hours of flooding, a
19 period of enhanced N₂O emissions occurred in all treatments. The unamended model soils with macroaggregates
20 emitted significantly more N₂O during this period than those with microaggregates. Litter addition modulated the
21 temporal pattern of the N₂O emission, leading to short-term peaks of high N₂O fluxes at the beginning of the
22 period of enhanced N₂O emissions. The presence of *S. viminalis* strongly suppressed the N₂O emission from the
23 macroaggregated model soil, masking any aggregate size effect. Integration of the flux data with data on soil
24 bulk density, moisture, redox potential and soil solution composition suggest that macroaggregates provided
25 more favorable conditions for spatially coupled nitrification–denitrification, which are particularly conducive to
26 net N₂O production, than microaggregates. The local increase in organic carbon in the detritosphere appears to
27 first stimulate N₂O emissions, but ultimately, respiration of the surplus organic matter shifts the system towards
28 redox conditions where N₂O reduction to N₂ dominates. Similarly, the low emission rates in the planted soils can
29 be best explained by root exudation of low-molecular weight organic substances supporting complete
30 denitrification in the anoxic zones, but also by the inhibition of denitrification in the zone above, where
31 rhizosphere aeration takes place. Together, our experiments highlight the importance of microhabitat formation
32 in regulating O₂ content and the completeness of denitrification in soils during drying after saturation. Moreover,
33 they will help to better predict the conditions under which hotspots and moments of enhanced N₂O emissions are
34 most likely to occur in hydrologically dynamic soil systems like floodplain soils.

35



36 1. Introduction

37 Nitrous oxide (N₂O) is a potent greenhouse gas with a global warming potential over a 100 year time horizon
38 298 times higher than the one of carbon dioxide (Forster et al., 2007). Given its role as climate-relevant gas and
39 in the depletion of stratospheric ozone (Ravishankara et al., 2009), the steady increase of its average atmospheric
40 concentration of 0.75ppb yr⁻¹ (Hartmann et al., 2013) asks for a quantitative understanding of its sources and the
41 factors that control its production. On a global scale, vegetated soils are the main natural terrestrial sources of
42 N₂O. Agriculture is the main anthropogenic source and the main driver of increasing atmosphere N₂O
43 concentrations (Ciais et al., 2013).

44 In soils, several biological nitrogen (N) transformation processes produce N₂O either as a mandatory
45 intermediate or as a by-product (Spott et al., 2011). Under oxic conditions, the most important process is obligate
46 aerobic nitrification that yields N₂O as by-product when hydroxylamine decomposes (Zhu et al., 2013). Under
47 low oxygen (O₂) availability, nitrifier denitrification and heterotrophic denitrification with N₂O as intermediate
48 become more relevant (Philippot et al., 2009). At stably anoxic conditions and low concentrations of nitrate,
49 complete denitrification consumes substantial amounts of previously produced N₂O by further reduction to N₂
50 (Baggs, 2008; Vieten et al., 2009). In environments that do not sustain, stable anoxia but undergo sporadic
51 transitions between oxic and anoxic conditions, the activity of certain N₂O reductases can be suppressed by
52 transiently elevated O₂ concentration and thus can lead to the accumulation of N₂O (Morley et al., 2008).

53 Nitrous oxide emissions from soils depend on the availability of carbon (C) and N substrates that fuel the
54 involved microbial processes. On the other hand, given its dependency on O₂, N₂O production is also governed
55 by the diffusive supply of O₂ through soils. Similarly, soil N₂O emissions are modulated by diffusive N₂O
56 transport from the site of production to the soil surface (e.g. Böttcher et al., 2011; Heincke and Kaupenjohann,
57 1999). Substrate availability, gas diffusivity, and the distribution of soil organisms are highly heterogeneous in
58 soils at a small scale, with micro-niches in particular within soil aggregates, within the detritosphere, and within
59 the rhizosphere. These can result in “hot spots” with high denitrification activity (Kuzuyakov and Blagodatskaya,
60 2015).

61 Soil aggregate formation is a key process in building soil structure and pore space. Soil aggregates undergo
62 different stages in their development, depending on the degradability of the main binding agent (Tisdall and
63 Oades, 1982). Initially, highly persistent primary organo–mineral clusters (20–250 μm) are held together by root
64 hairs and hyphae, thus forming macroaggregates (> 250 μm). Upon decomposition of these temporary binding
65 agents and the subsequent disruption of the macroaggregates, microaggregates (< 250 μm) are released (Elliott
66 and Coleman, 1988; Oades, 1984; Six et al., 2004). These consist of clay-encrusted fragments of organic debris
67 coated with polysaccharides and proteins. This multi-stage development leads to a complex relationship between
68 aggregate size, intra-aggregate structure and soil structure (Ball, 2013; Totsche et al., 2017), which influences
69 soil aeration, substrate distribution and pore water dynamics (Six et al., 2004). Often, micro-site heterogeneity
70 increases with aggregate size, thus fostering the simultaneous activity of different N₂O producing microbial
71 communities with distinct functional traits (Bateman and Baggs, 2005). Aggregate size effects on N₂O
72 production and consumption have generally been studied in static batch incubation experiments with a
73 comparatively small number of isolated aggregates of uniform size, at constant levels of water saturation (Diba
74 et al., 2011; Drury et al., 2004; Jahangir et al., 2011; Khalil et al., 2005; Sey et al., 2008), and through modelling
75 approaches (Renault and Stengel, 1994; Stolk et al., 2011). Previous work provided partially inconsistent results,



76 which led to an ongoing discourse about the interplay of physicochemical properties and different aggregate
77 sizes in controlling N_2O emission. For example, ostensible inconsistencies may be attributed to the use of
78 different aggregate size classes, other methodological constraints (water saturation, redox potential), and
79 differences in microbial communities. The effects of aggregate size, in combination with fluctuating water
80 saturation, on soil N_2O emissions have, to our knowledge, not been addressed specifically.

81 Similar to soil aggregates, the detritosphere and the rhizosphere (the zone of the soil that is affected by root
82 activity (Baggs, 2011; Luster et al., 2009), can be considered biogeochemical hot spots (Kuzyakov and
83 Blagodatskaya, 2015; Myrold et al., 2011). Here, carbon availability is much higher than in the bulk soil and
84 thus rarely limiting microbial process rates. The detritosphere consists of dead organic material, which spans a
85 wide range of recalcitrance to microbial decomposition. Spatially confined accumulations of variably labile soil
86 litter form microhabitats that are often colonized by highly active microbial communities (Parkin, 1987).
87 Aggregation of litter particles has been shown to affect N_2O emissions (Loecke and Robertson, 2009). Hill
88 (2011) identified buried organic-rich litter horizons in a stream riparian zone as hot spots of N cycling. Similarly,
89 in the rhizosphere, root exudates and exfoliated root cells provide ample degradable organic substrate for soil
90 microbes (Robertson and Groffman, 2015). Yet, plant growth may also affect soil microbial communities
91 through competition for water and nutrients (e.g., fixed N) (Bender et al., 2014; Myrold et al., 2011). The
92 combined effects of these plant-soil interactions on N_2O production have been reviewed by Philippot et al.
93 (2009). Root-derived bioavailable organic compounds can stimulate heterotrophic microbial activity, specifically
94 N mineralization and denitrification. Nitrification in turn can be enhanced by the elevated N turnover and
95 mineralization rates, but may also be negatively affected by specific inhibitors released from the root or through
96 plant-driven ammonium depletion. The ability of some plants adapted to water-saturated conditions to
97 „pump“ air into the rhizosphere via aerenchyma (gas conductive channels in the root) leads to an improved
98 oxygenation of the rhizosphere and a stimulation of nitrification (Philippot et al., 2009). Surrounded by
99 otherwise anoxic sediments, such aerated micro-environments may create optimal conditions for coupled
100 nitrification–denitrification (Baldwin and Mitchell, 2000; Koschorreck and Darwich, 1998). On the other hand,
101 transport of N_2O produced in the soil to the atmosphere is may be facilitated via these plant-internal channels,
102 bypassing diffusive transport barriers and enhancing soil–atmosphere gas fluxes (Jørgensen et al., 2012).

103 The dynamics of N_2O emissions are strongly coupled to the dynamics of pore water. Re-wetting of previously
104 dried soil can lead to strong N_2O emissions (Goldberg et al., 2010; Ruser et al., 2006), likely fostered by a
105 wetting-induced flush in N mineralization (Baldwin and Mitchell, 2000). On the other hand, the drying-phase
106 after water saturation of sediments and soils can lead to a period of enhanced N_2O emissions (e.g. Baldwin and
107 Mitchell, 2000; Groffman and Tiedje, 1988; Rabot et al., 2014; Shrestha et al., 2012) when water-filled pore
108 space (WFPS) exceeds 60% (Beare et al., 2009; Rabot et al., 2014). The increased N_2O production has been
109 attributed to enhanced coupled nitrification–denitrification (Baldwin and Mitchell, 2000). Depending on the
110 spatial distribution of water films around soil particles and tortuosity (which is a function of aggregate size and
111 soil structure), the uneven drying of the soil after full saturation may generate conditions that are conducive to
112 the formation of anaerobic zones in otherwise oxic environments (Young and Ritz, 2000). Pore water thereby
113 acts as a diffusion barrier for gas exchange, limiting the O_2 availability in the soil pore space (Butterbach-Bahl
114 et al., 2013). Moreover, pore water serves as a medium for the diffusive dispersal of dissolved C and N substrates,
115 e.g. from the site of litter decomposition to spatially separated N_2O producing microbial communities (Hu et al.,
116 2015). Therefore, fluctuations in water saturation efficiently promote the development of hot spots and hot



117 moments of N₂O emissions in floodplain soils and other semi-terrestrial soils (Hefting et al., 2004; Shrestha et al.,
118 2012).
119 The main objective of the present experimental study was to contribute to a better understanding of the factors
120 governing the formation and emission of N₂O in floodplain soils during hot moments after flooding events.
121 Towards this objective, we performed a mesocosm flooding simulation experiment under controlled conditions,
122 with model soils of largely similar structure, but differing in the size distribution of original soil aggregates. We
123 included two additional factorial treatments: a willow-litter addition treatment to assess whether aggregate size
124 effects are modified by such a detritosphere, and a willow cuttings treatment to test whether aggregate effects
125 change in the presence of plants, as result of root soil interactions.
126 We demonstrate that the level of soil aggregation affects N₂O emission rates from floodplain soils through its
127 modulating control on the model soils physicochemical properties. We further show that these effects are
128 modified by the presence of a detritosphere and by root–soil interactions, through effects on carbon and N
129 substrate availability and redox conditions.

130 2. Material and methods

131 2.1 Model soils

132 In February 2014, material from the uppermost 20 cm of a N-rich gleyic Fluvisol (calcaric, humic siltic) with
133 20% sand and 18% clay (Samaritani et al., 2011) was collected in the restored Thur River floodplain near
134 Niederneunforn (NE Switzerland 47°35' N, 8°46' E, 453 m.a.s.l.; MAT 9.1 °C; MAP 1015 mm). After removing
135 plant residues such as roots, twigs and leaves, the soil was mixed and air-dried to a gravimetric water content of
136 24.7 ± 0.4 %. In the next step, the floodplain soil material was separated into a macroaggregate fraction (250–
137 4000 µm) and a microaggregate fraction (< 250 µm) by dry sieving. The threshold of 250 µm between
138 macroaggregates and microaggregates was chosen based on Tisdall and Oades (1982). Soil aggregate fractions
139 were then used to re-compose model soils. In order to preserve the original soil structure, the remaining
140 aggregate size fractions were complemented with an inert matrix replacing the removed aggregate size fraction
141 of the original soil. Model Soil 1 (LA) was composed of soil macroaggregates mixed in a 1:1 (w/w) ratio with
142 glass beads of 150–250 µm size serving as inert matrix material replacing the microaggregates of the original
143 soil. Similarly, Model Soil 2 (SA) was composed of soil microaggregates mixed at the same ratio with fine
144 quartz gravel of 2000–3200 µm size. To generate an even mixture of original soil aggregates and the respective
145 inert matrix a Turbula mixer (Willy A. Bachofen AG, Muttenz, Switzerland) was used. The physicochemical
146 properties of the two soils were determined by analysing three random samples of each model soil. Texture of
147 the complete model soils was determined using the pipette method (Gee and Bauder, 1986) and pH was
148 measured potentiometrically in a stirred slurry of 10 g soil in 20 ml of 0.01 M CaCl₂. Additionally C_{org} and N_{tot}
149 were analysed in both aggregate size fractions without the inert material, using the method described by Walthert
150 et al. (2010). The two model soils displayed very similar physicochemical properties (Table 1), except for the
151 C:N ratio that was lower in macroaggregates than in microaggregates. The latter was due to the slightly lower
152 organic carbon content in concert with slightly higher N_{tot} values in the macroaggregates. The high calcium
153 carbonate (CaCO₃) content of the source material of our model soils (390 ± 3 g CaCO₃ kg⁻¹; Samaritani et al.,
154 2011) buffered the systems at an alkaline pH of 8.00 ± 0.02 for LA and 7.56 ± 0.01 for SA respectively (Table 1),
155 ensuring that the activity of key N-transforming enzymes was not hampered by too low pH, and that the potential



156 for simultaneous production and consumption of N₂O in our experiment was fully intact (Blum et al., 2018;
157 Frame et al., 2017).

158 2.2 Mesocosms

159 For the mesocosm experiments, transparent polyvinyl chloride (PVC) cylinders with polymethyl methacrylate
160 (PMMA) couplings were used. A mesocosm comprised a bottom column section, containing the soil material
161 and a drainage layer as described below, and the upper headspace section with a detachable headspace chamber
162 (Fig. 1). Each column section was equipped with two suction cups (Rhizon MOM Soil Moisture Samplers,
163 Rhizosphere Research Products, Netherlands; pore size 0.15 µm) for soil solution sampling. The suction cups
164 were horizontally inserted at 5 cm and 20 cm below soil surface. For redox potential measurements, two custom-
165 made Pt electrodes (tip with diameter of 1 mm and contact length of 5 mm) were placed horizontally at a 90°
166 angle to the suction cups at the same depths, with the sensor tip being located 5 cm from the column wall. A
167 Ag/AgCl reference electrode (B 2820, SI Analytics, Germany) was installed as shown in Fig. 1. A volumetric
168 water content (VWC) sensor (EC-5, Decagon, USA) was installed 15 cm below the soil surface. To avoid
169 undesired waterlogging, each column section contained a 5 cm thick drainage layer composed of quartz sand
170 with the grain size decreasing with depth from 1 mm to 5.6 mm (Fig. 1). The upper cylinder section was
171 equipped with three way valves for gas sampling, and an additional vent for pressure compensation.

172 2.3. Experimental setup

173 The mesocosm experiment had a two factorial design where factor 1 (model soil) had two levels
174 (macroaggregates or microaggregates) and factor 2 (treatment) had three levels (unamended, litter addition and
175 plant presence) resulting in six treatments, each replicated six times (Table 2). As basic material, each mesocosm
176 contained 8.5 kg of either of the two model soils. Unamended model soils were used to investigate exclusively
177 the effect of aggregate size, abbreviated as LAU (large aggregates unamended) and SAU (small aggregates
178 unamended), respectively. In order to assess detritusphere effects, two sets of mesocosms were amended with
179 freshly collected leaves of Basket Willow (*Salix viminalis* L.). Those leaves were cut into small pieces,
180 autoclaved, and then added to the model soil components (8 g kg⁻¹ model soil) during the mixing procedure to
181 create treatments LAL (large aggregates litter) and SAL (small aggregates litter), respectively. A third set of
182 mesocosms was planted with cuttings collected from the same basket willow (*Salix viminalis* L.) to evaluate the
183 effects of root–soil interactions in the respective model soils. For each mesocosm (treatments LAP/large
184 aggregate plants and SAP/small aggregates plants, respectively) one cutting was inserted 10 cm into the soil,
185 protruding from the surface about 3 cm.

186 The addition of leaf litter to the model soils led to an increase of C_{org} and total nitrogen (TN) in LAL relative to
187 LAU by 41 % and 35 %, respectively, and in SAL relative to SAU by 58 % and 44 % respectively. The bulk
188 density of the unamended model soil SAU (1.27 ± 0.01 g cm⁻³) was slightly higher than the one of LAU (1.22 ±
189 0.01 g cm⁻³; adj. *P*: < 0.0001). Regarding the litter addition treatments, the bulk density of LAL (1.13 ± 0.01 g
190 cm⁻³) was significantly smaller than the one of LAU (adj. *P*: < 0.0001), whereas the bulk density of SAL (1.27 ±
191 0.02 g cm⁻³) did not differ significantly from the one of SAU. The soils in the treatments with plants exhibited a
192 similar bulk density (LAP: 1.23 ± 0.02 g cm⁻³; SAP: 1.24 ± 0.01 g cm⁻³) as in the respective unamended
193 treatments.



194 The experiments were conducted inside a climate chamber set to constant temperature (20 ± 1 °C) and relative
195 air humidity ($60 \pm 10\%$), with a light/dark cycle of 14/10 h (PAR 116.2 ± 13.7 $\mu\text{mol m}^{-2} \text{s}^{-1}$). The experimental
196 period was divided into four consecutive phases: The conditioning phase (phase 1) lasted for 15 weeks and
197 allowed the model soils to equilibrate and the plants to develop a root system. This was followed by the first
198 experimental phase of nine days (phase 2), serving as a reference period under steady-state conditions. During
199 phases 1 and 2, the soils were continuously irrigated with artificial river water (Na^+ : 0.43 μM ; K^+ : 0.06 μM ;
200 Ca^{2+} : 1.72 μM ; Mg^{2+} : 0.49 μM ; Cl^- : 4.04 μM ; NO_3^- : 0.16 μM ; HCO_3^- : 0.5 μM ; SO_4^{2-} : 0.11 μM ; pH: 7.92) via
201 suction cups, to maintain a volumetric water content of 35 ± 5 %. In phase 3, the mesocosms were flooded by
202 pumping artificial river water through the drainage vent at the bottom into the cylinder (10 mL min^{-1} , using a
203 peristaltic pump; IPC-N-24, Ismatec, Germany) until the water level was 1 cm above the soil surface. After 48 h
204 of flooding, the water was allowed to drain and the soil to dry for 18 days without further irrigation (phase 4).

205 2.4 Sampling and analyses

206 During the entire experiment, water content and redox potential were automatically logged every 5 minutes
207 (EM5b, Decagon, USA and CR1000, Campbell scientific, USA, respectively).

208 At selected time points during the experiment, soil-emitted gas and soil solution were sampled. For N_2O flux
209 measurements, 20, 40 and 60 minutes after closing the mesocosms, headspace gas samples (20 mL) were
210 collected using a syringe and transferred to pre-evacuated exetainers. The samples were analyzed for their N_2O
211 concentration using a gas chromatograph (Agilent 6890, Santa Clara, USA; Porapak Q column, Ar/ CH_4 carrier
212 gas, micro-ECD detector). Measured headspace N_2O concentrations were converted to moles using the ideal gas
213 law and headspace volume. The N_2O efflux rates were calculated as the slope of the linear regression of the N_2O
214 amounts at the three sampling times, relative to the exposed soil surface area (Fig. 1, Shrestha et al., 2012).

215 For soil water sampling, 20 mL of soil solution were collected using the suction cups. Water samples were
216 analyzed for dissolved organic carbon (DOC) and TN concentrations with an elemental analyzer (Formacs^{HT/TN},
217 Skalar, The Netherlands). Nitrate and ammonium concentrations were measured by ion chromatography (IC 940,
218 Metrohm, Switzerland), and nitrite concentrations were determined photometrically (DR 3900, Hach Lange,
219 Germany).

220 2.5 Data analyses

221 Differences among the six treatments on individual sampling dates in N_2O fluxes, DOC and N-species
222 concentrations in soil solution were tested for significance using the non-parametric Kruskal–Wallis test
223 followed by Dunn’s post hoc test. To estimate the total amount of N_2O emitted during the period of enhanced
224 N_2O fluxes in phase 4, Q_{tot} , the N_2O fluxes between day 11 and 25 of the experiment were integrated as follows:

$$225 \quad Q_{\text{tot}} = \frac{1}{2} \sum_{n=1}^{n_{\text{max}}} [\Delta_n \times (q_n + q_{n+1})], \quad (1)$$

226 where Δ_n is the time period between the n^{th} and the $n+1^{\text{th}}$ measurement, and q_n and q_{n+1} the mean flux on the n^{th}
227 and $n+1^{\text{th}}$ measurement day, respectively. “ $n=1$ ” refers to day 11, and n_{max} to day 25 of phase 4. The integrated
228 N_2O flux data were tested for differences between treatments and model soils by performing a two way ANOVA
229 and the Tukey’s honestly significant difference (HSD) post hoc test. No data transformation was necessary, since
230 the inspection of residuals of the ANOVA model and the application of the Shapiro–Wilk normality test revealed



231 that the values follow a Gaussian distribution. Significance and confidence levels were set at $\alpha < 0.05$. For the
232 statistical analyses we used Graphpad Prism (GraphPad Software Inc., 2017) and R (R Core Team, 2018).

233 3. Results

234 3.1 Soil moisture and redox potential

235 During phase 1 and 2, saturation levels stabilized at $53.0 \pm 2.1\%$ WFPS (water filled pore space) in the
236 treatments with LA soils, and were slightly higher in SA treatments ($57.8 \pm 2.0\%$) (Fig. 2). The flooding of the
237 mesocosms for 48 h with artificial river water raised the WFPS for all LA soils to $87.8 \pm 0.1\%$, significantly
238 exceeding the increase of WFPS in SA soils ($80.6 \pm 0.1\%$). The water release from the system after the
239 simulated flood resulted in an immediate drop of the WFPS, except for the LAU treatment (Fig. 2). This was
240 followed by slow drying for 1 week, and a more marked decrease in WFPS during the second week after the
241 flood. During the latter period, the plant treatments dried faster than the other treatments. As a result, at the end
242 of the experiment, WFPS was still above pre-flood values in unamended and litter treatments, while WFPS
243 levels in the treatments with plants were lower than before the flooding.

244 The time course of the redox potential measured in 5 cm and 20 cm depth exhibited distinct patterns depending
245 on the respective model soil (Fig. 3). In all treatments, flooding induced a rapid decrease of the redox potential to
246 values below 250 mV within 36 hours. Upon water release, the redox potential returned rapidly to pre-flood
247 values at both measurement depths only in SA soils. In the LA treatments (most pronounced in LAL), soils at 20
248 cm depth underwent a prolonged phase of continued reduced redox condition, returning to the initial redox levels
249 only towards the end of the experiment.

250 3.2 Hydrochemistry of soil solutions

251 Considering individual treatments, DOC concentrations varied only little with time. Yet, the DOC concentrations
252 were generally much higher in treatments with LA than with SA soils. Nitrate was the most abundant dissolved
253 reactive N species in the soil solution, with pre-flood concentrations of 1 to 5 mM (Fig. 4d–f). In the unamended
254 and plant treatments, NO_3^- concentrations were markedly higher in SA than in LA soils, whereas they were
255 similar in both litter addition treatments. Two distinct temporal patterns in the evolution of NO_3^- concentration
256 could be discerned. In the unamended and litter-addition treatments, NO_3^- concentrations decreased after the
257 flooding, consistently reaching a minimum on day 19, in the case of the litter treatments below the detection
258 limit of 0.2 μM , before increasing again during the later drying phase (Fig 4d,e). In contrast, in the treatments
259 with plants, NO_3^- concentrations steadily declined from concentrations of 1–2 mM to around 0.5 mM at the end
260 of the experiment (Fig. 4f). Nitrite was found at significant concentrations only in LA soils, with highest
261 concentrations in the LAU treatment right after the flooding (33.6 μM) and decreasing concentrations throughout
262 the remainder of the experiment (Fig. 4g–i). In SA soils NO_2^- concentration was always $< 5 \mu\text{M}$, without much
263 variation. Similarly, in most treatments except SAL, ammonium (NH_4^+) concentrations were $< 10 \mu\text{M}$, and
264 particularly towards the end of the experiment very close to the detection limit (Fig. 4j, 4l). In the SAL treatment,
265 NH_4^+ concentrations peaked 5 d after the flood with concentrations of around 70 μM (Fig. 4k).

266 3.3 Nitrous oxide emissions



267 During phase 2 (i.e., before the flooding), N₂O fluxes were generally low (< 1 μmol m⁻² h⁻¹; Fig. 2), however,
268 fluxes in the LAL treatment were significantly higher than in the other treatments (adj. P = 0.002–0.039; Fig. 2).
269 The flooding triggered the onset of a “hot moment”, defined here as period with strongly increased N₂O
270 emissions, which lasted for about one week independent of the treatment (Fig. 2). The maximum efflux was
271 observed immediately after the flood. The subsequent decline in N₂O emission rates followed different patterns
272 among the various treatments. Normalizing the N₂O flux to the maximum measured efflux for each replicated
273 treatment revealed a slower decrease with time for the unamended soils than for the litter and plant treatments
274 (not shown). The strongest peak emissions were observed in the LAL treatment (91.6 ± 14.0 μmol m⁻² h⁻¹; mean
275 ± SD). Throughout most of the drying phase, the LAU and LAL treatments exhibited higher N₂O emissions than
276 the corresponding SAU and SAL experiments. In contrast, there was no such difference in the treatments with
277 plant cuttings, and peak N₂O emissions were overall lower than in the other treatments. The integrated N₂O
278 fluxes during the hot moment (days 10 to 25 of the experiment) were significantly higher for the LAU and LAL
279 than for all other treatments (Fig. 5). Again, there was a significant aggregate size effect in the unamended (adj.
280 P = 0.045) and litter-addition treatments (adj. P = 0.008). The integrated N₂O emissions in the two plant
281 treatments did not differ significantly from each other, but were significantly smaller than in the LAU (adj. P =
282 0.001), and the LAL (adj. P = 0.005) treatments.

283 4. Discussion

284 In our experiment, we could confirm the occurrence of periods of enhanced N₂O emissions in the drying phase
285 shortly after flooding, as expected based on previous research (Baldwin and Mitchell, 2000; Groffman and
286 Tiedje, 1988; Rabot et al., 2014; Shrestha et al., 2012). We observed that the six treatments had a substantial
287 effect on the magnitude and temporal pattern of N₂O emissions that could only be captured by observations at
288 relatively high temporal resolution. The fast occurrence of strong N₂O fluxes over a comparatively short period
289 in the litter-amended treatment on the one side, and the relatively weak response to the flooding in the plant
290 treatment on the other, suggests complex interactive mechanisms related to distinct microhabitat effects leading
291 to characteristic periods of enhanced N₂O emission. Rabot et al. (2014) explained N₂O emission peaks during the
292 desaturation phase with the release of previously produced and entrapped N₂O. Such a mechanism may partly
293 contribute to high N₂O emissions in our experiment initially, but the continuing depletion of NO₃⁻ and NO₂⁻
294 during the phase of high N₂O emissions indicates that the flooding and drying has strong effects on N
295 transformations mediated by microorganisms in the soil (e.g., the balance and overall rates of nitrification,
296 nitrifier–denitrification, and denitrification). Hence, physical controls alone clearly do not explain the observed
297 timing and extent of hot moments with regard to N₂O emission. In the following sections we will discuss how
298 the effect of flooding on microbial N₂O production is modulated by differential microhabitat formation (and
299 hence redox conditions) in the various treatments.

300 4.1 Effect of aggregate size on N₂O emissions

301 Our results indicate that aggregate size is a major factor in modulating soil N₂O emissions. In the unamended
302 and litter addition treatments, LA model soils exhibited both higher peak and total N₂O emissions during the hot
303 moment in the drying phase than SA model soils (Figs. 2 and 5). By contrast, in the presence of a growing
304 willow, there was no detectable effect of aggregate size on the overall N₂O emission (further discussion below).



305 The aggregate size effects observed in the unamended and litter treatments can be explained by factors
306 controlling (i) gas diffusion (e.g. water film distribution, tortuosity of the intra-aggregate pore space) and (ii)
307 decomposition of encapsulated SOM regulating the extent of N_2O formation (Neira et al., 2015). In order to
308 isolate the effect of aggregate size (i.e., to minimize the effect of other factors that are likely to influence gas
309 diffusion), we created model soils of similar soil structure (see Materials and Methods). The results of the
310 particle size analysis confirmed a nearly identical texture of the two model soils, and at least in the unamended
311 treatments a similar bulk density was achieved. The effect of soil texture and structure should therefore be
312 similar for both model soils. The same applies to bulk soil chemical properties of the two aggregate size fractions
313 such as C_{org} content and pH. Therefore, we assume in the following that the differences in N_2O emissions among
314 the treatments can mainly be attributed to size-related aggregate properties and their interactions with litter
315 addition or rhizosphere effects.

316 During phase 3 with near-saturated conditions, no aggregate size effect was observed. High WFPS seem to have
317 limited the gas diffusion (O_2 and N_2O) independent of the aggregate size, limiting soil–atmosphere gas exchange
318 in both model soils equally (Neira et al., 2015; Thorbjørn et al., 2008). As a consequence of inhibited gas
319 exchange/soil aeration, a sharp drop in the redox potential was observed in all treatments, indicating a rapid
320 decline in O_2 availability to suboxic/anoxic conditions. Together with an incipient decrease in soil solution NO_3^- ,
321 this indicates that N_2O production is primarily driven by denitrification in this phase.

322 The aggregate size effects on the formation of moments of enhanced N_2O emission became evident during the
323 subsequent drying period. During the initial drying phase, when a heterogeneous distribution of water films
324 around soil particles/aggregates develops (Young and Ritz, 2000), the macroaggregates in the LA model soils
325 appear to foster micro-environmental conditions that are more beneficial to N_2O production. This could be
326 related to the longer diffusive distances for re-entering O_2 caused by the higher tortuosity of the intra-aggregate
327 pore space of macroaggregates, as reported by Ebrahimi and Or (2016). This may have helped to maintain, or
328 even extend, reducing conditions due to microbial activity inside the core of macroaggregates during drying.
329 Thus, on the one hand, large aggregates favor the emergence of anoxic microhabitats expanding the zones where
330 denitrification occurs. On the other hand, the overall higher porosity of the LA soils supports a better aeration in
331 drained parts of the soil (Sey et al., 2008), and aerobic processes (e.g., nitrification) are supported. As a result,
332 ideal conditions for spatially coupled nitrification–denitrification are created (Baldwin and Mitchell, 2000;
333 Koschorreck and Darwich, 1998). Indeed, the emergence of heterogeneously distributed, spatially confined
334 oxygen minimum zones during soil drying may be reflected by the high variability of the redox conditions
335 observed in replicate mesocosms and, on average, the tendency towards lower redox potentials for a prolonged
336 period of time in the subsoils of the LA model soils (Fig. 3 d–f). In this context, the relevance of water films for
337 the emergence of periods of enhanced N_2O emissions is further highlighted by the fact that elevated flux rates
338 were only observed as long as the WFPS was above 65%. This is consistent with work by Rabot et al. (2014)
339 and Balaine et al. (2013), who found similar soil water saturation thresholds for elevated N_2O emissions from
340 soils, attributing this phenomenon to suboptimal environmental conditions for both nitrification and
341 denitrification at lower saturation levels.

342 Given the arguments above, we assume that N_2O emissions during the drying phase originate to a large degree
343 from heterotrophic denitrification, and that they are governed mainly by the aggregate size dependent redox
344 conditions within the semi-saturated soils. This conclusion stands in good agreement with findings from Drury et
345 al. (2004) who found higher production of N_2O due to enhanced denitrification with increasing size of intact



346 arable soil aggregates in a laboratory incubation study. In contrast, the much lower emissions from the SA
347 treatments can best be explained by a rapid return to pre-flood, i.e. oxic, conditions in most of the pore space,
348 under which N₂O production driven by denitrification is inhibited. According to Manucharova et al. (2001) and
349 Renault and Stengel (1994), aggregates smaller than 200 µm are simply not large (and reactive) enough (i.e.,
350 molecular diffusive distances for oxygen are too short) to develop suboxic or anoxic conditions in the center, let
351 alone denitrifying zones. Hence, only a relatively small fraction of the total number of microaggregates in the SA
352 soils would have been large enough (between 200 and 250 µm) to host denitrification and act as site of anaerobic
353 N₂O production.

354 4.2 Litter effect on N₂O emissions

355 We expected that litter addition would increase N₂O emissions from model soils with both small and large
356 aggregates, as was found earlier (e.g. Loecke and Robertson, 2009; Parkin, 1987). The addition of litter to the
357 model soils changed the temporal dynamics of the N₂O emission substantially, but its effect on the net integrated
358 N₂O emission was rather minor (Fig. 5). More precisely, highest peak emission rates of all treatments were
359 observed in the LAL treatment, but peak emission rates were followed by a faster return to low pre-flood
360 emission rates in the LAL and the SAL treatments relative to the unamended treatments (Fig 2). This confirms
361 that surplus organic carbon can, on short-term, boost N₂O emissions, particularly in the large-aggregate
362 treatment. The fast mid-term return to low N₂O emission suggests that N₂O production by heterotrophic
363 denitrification either becomes limited by substrates other than carbon, and/or that the carbon added to the soils
364 affects the redox-biogeochemistry in a way that shifts the balance between N₂O production and consumption in
365 favor of consumption. Loecke and Robertson (2009) reported similar temporal N₂O emission patterns in field
366 experiments with litter-amended soil, and attributed the observed dynamic of a rapid decline after peak emission
367 to an increased demand for terminal electron acceptors during denitrification shortly after the carbon addition.
368 Nitrate/nitrite limitation leads, under stable anoxic conditions, ultimately to the complete reduction of produced
369 N₂O to N₂ decreasing net N₂O emission. Indeed, the rapid decrease in N₂O emissions after the emission rate peak
370 in the litter addition treatments was accompanied by the complete depletion of NO₃⁻ in the soil solution at low
371 redox potential, suggesting nitrate limitation. The increased demand for electron acceptors can be attributed to
372 the increased availability of labile C compounds and nutrients provided by the mineralization of litter, and the
373 concomitant stimulation of aggregate-associated microbial communities during the flooding (Li et al., 2016). At
374 the same time, the litter-stimulated soil respiration increases the soil's oxygen demand, maintaining stable low
375 redox conditions for a longer period of time during the drying phase. Since high activity of N₂O reductase
376 requires very low O₂ concentrations (Morley et al., 2008), such conditions may be particularly favorable for
377 complete denitrification to N₂, an additional, or alternative, explanation for the low N₂O emission rates shortly
378 after the N₂O emission peak.

379

380 4.3 Effects of *Salix viminalis*

381 Planted willow cuttings resulted in relatively low maximum N₂O emission rates (LAP: 19.75 ± 9.31 µmol m⁻² h⁻¹;
382 ¹; SAP: 15.07 ± 12.07 µmol m⁻² h⁻¹; mean ± SD), independent of aggregate size. The high values for WFPS
383 throughout the hot moment, and a low redox potential in the subsoil, imply optimal conditions for denitrification
384 or nitrifier denitrification, but compared to unamended and litter-addition treatments, only little N₂O was emitted



385 (both during peak N₂O emission rates and with regards to the integrated N₂O flux). *S. viminalis* suppressed peak
386 N₂O emissions, overriding the positive effect of large aggregates on N₂O emissions observed otherwise. The
387 specific mechanisms involved are uncertain. Fender et al. (2013) found in laboratory experiments with soil from
388 a temperate broad-leaved forest planted with ash saplings N₂O fluxes and plant effects very similar to the ones
389 observed in our study. They attributed reduced N₂O emissions in presence of ash partly to plant uptake of
390 nutrients that reduced NO₃⁻ availability to denitrifiers. Fast-growing plant species like *Salix* are particularly
391 effective in removing soil inorganic N (Kowalik and Randerson, 1994). Such a causal link between reduced N₂O
392 emissions and plant growth is, however, not supported by our data. More precisely, the NO₃⁻ concentrations
393 during the hot moment of N₂O emissions were always relatively high (> 0.5 mM) and above the levels observed
394 in the litter treatments.

395 An alternative explanation for the reduced N₂O emissions in the plant treatments could be rhizosphere aeration
396 by aerenchyma, a physiological trait of *Salix viminalis* roots, which prevents the formation of anoxia in their
397 close vicinity (Blom et al., 1990; Randerson et al., 2011). Thus, while aerenchyma in general aid in the gas
398 exchange between the soil and the atmosphere, and would per se accelerate transport of N₂O from soils to the
399 atmosphere, they also inhibit anaerobic N₂O production by aerating the rhizosphere. Indeed, redox potentials in
400 the topsoil were higher in SAP and LAP compared to the other treatments. By contrast, the redox potential in the
401 saturated subsoil below was even lower than observed for the unamended soils. This indicates that the aeration
402 effect by aerenchyma is constrained to the upper soil, or is, in the deeper soil portions, compensated by
403 respiratory rhizosphere processes. According to Fender et al. (2013), in vegetated soils, microbial respiration is
404 stimulated by deposition of root exudates, which in concert with root respiration in a highly saturated pore space,
405 leads to severe and ongoing oxygen depletion. Again, N₂ and not N₂O is the dominant final product of
406 denitrification, under the stable anoxic condition produced this way, and N₂O emissions will be low.

407 5. Conclusions

408 In this study, we investigated the distinct effects of aggregate size, surplus organic carbon from litter and
409 vegetation on N₂O emission from model soils after flooding. Flooding and drying were always associated with
410 hot moments of N₂O production, most likely due to heterotrophic denitrification as result of suboxic O₂ levels at
411 high WFPS. Our results demonstrate that aggregate size is a very important factor in modulating N₂O emission
412 from soils under changing pore space water saturation. Aggregates of a diameter > 250 μm appear to foster
413 suboxic microhabitats that favor denitrification and associated N₂O emission. This soil aggregate size effect may
414 be amplified in the presence of excess carbon substrate, as long as heterotrophic denitrification as the main N₂O
415 producing process is not electron acceptor limited, and extremely reducing conditions in organic rich soils do not
416 promote complete denitrification leading to a further reduction of N₂O to N₂. On the other hand, the higher
417 porosity of the soils with macroaggregates may aid in the formation of microsites at the surface of aggregates
418 where nitrification is re-initialized during drying, supporting favorable conditions for spatially coupled
419 nitrification–denitrification. The mechanisms by which processes in the rhizosphere of *Salix viminalis* effectively
420 suppress N₂O emissions, and thus mask any aggregate size effect, remain ambiguous. Distinct physiological
421 features of *Salix viminalis*, its root metabolism, in combination with microbial respiration can lead to the
422 simultaneous aeration of some parts of the rhizosphere, and the formation of strongly reducing zones in others.
423 In both cases, redox conditions seem to be impedimental for extensive net N₂O production.



424 Our results demonstrate the importance and complexity of the interplay between soil aggregate size, labile
425 organic C availability, respiratory processes in the rhizosphere, and plant-induced aeration of soils under
426 changing soil water content. Those interactions emerged as modulators of N₂O emissions by controlling the O₂
427 distribution in the soil matrix. Indeed, O₂ appears as the unifying master variable that ultimately sets the
428 boundary conditions for N₂O production and/or consumption.

429 The main scope of this work was to expand our knowledge on the controls on net N₂O emissions from floodplain
430 soils. The systematic relationships observed in this study are likely to help anticipating where and when hotspots
431 and hot moments of N₂O emissions are most likely to occur in hydrologically dynamic soil systems like
432 floodplain soils. Further understanding of the complex interaction between plants and soil microorganisms, the
433 detritusphere, and soil aggregation, as well as their influence on N turnover and N₂O accumulation in soils,
434 should focus on how the parameters tested affect the actual activity of the nitrifying and denitrifying
435 communities, with an in-depth investigation into the biogeochemical pathways involved.

436 *Data availability.* Data will be openly available at <https://datadryad.org/>

437 *Competing interests.* The authors declare that they have no conflict of interest.

438 *Authors contributions.* The initial concept of the experiment was developed by JL, MFL and PAN. ML planned
439 the experiment in detail, set it up and performed it. PAN supervised the measurement of N₂O gas concentrations,
440 whereas ML conducted all other measurements and data analyses. ML wrote the manuscript with major
441 contributions by JL, MFL and PAN.

442 *Acknowledgements.* The authors thank the Department of Evolutionary Biology and Environmental Studies of
443 the University of Zurich and René Husi for performing the GC measurements. We are also very grateful to the
444 Environmental Geoscience research group in the Department of Environmental Sciences of the University of
445 Basel and Judith Kobler–Waldis for helping us with the IC measurements. We thank the Central Laboratory and
446 Daniel Christen, Roger Köchli and Noureddine Hajjar of the Swiss Federal Institute for Forest, Snow and
447 Landscape Research (WSL) for assistance with chemical analyses. This study was funded by the Swiss National
448 Science Foundation (SNSF) under the grant number 200021_147002 as well as by financial resources of WSL
449 and the University of Basel.

450 **References**

- 451 Baggs, E. M.: A review of stable isotope techniques for N₂O source partitioning in soils: recent progress,
452 remaining challenges and future considerations, *Rapid Commun. Mass Spectrom.*, 22(11), 1664–1672,
453 doi:10.1002/rcm.3456, 2008.
- 454 Baggs, E. M.: Soil microbial sources of nitrous oxide: Recent advances in knowledge, emerging challenges and
455 future direction, *Curr. Opin. Environ. Sustain.*, 3(5), 321–327, doi:10.1016/j.cosust.2011.08.011, 2011.
- 456 Balaine, N., Clough, T. J., Beare, M. H., Thomas, S. M., Meenken, E. D. and Ross, J. G.: Changes in Relative
457 Gas Diffusivity Explain Soil Nitrous Oxide Flux Dynamics, *Soil Sci. Soc. Am. J.*, 77(5), 1496–1505, doi:DOI



- 458 10.2136/sssaj2013.04.0141, 2013.
- 459 Baldwin, D. S. and Mitchell, A. M.: The effects of drying and re- flooding on the sediment and soil nutrient
460 dynamics of lowland river–floodplain systems: a synthesis, *Regul. Rivers Res. Manag.*, 16(5), 457–467,
461 doi:10.1002/1099-1646(200009/10)16:5<457::AID-RRR597>3.3.CO;2-2, 2000.
- 462 Ball, B. C.: Soil structure and greenhouse gas emissions: A synthesis of 20 years of experimentation, *Eur. J. Soil*
463 *Sci.*, 64(3), 357–373, doi:10.1111/ejss.12013, 2013.
- 464 Bateman, E. J. and Baggs, E. M.: Contributions of nitrification and denitrification to N₂O emissions from soils
465 at different water-filled pore space, *Biol. Fertil. Soils*, 41(6), 379–388, doi:10.1007/s00374-005-0858-3, 2005.
- 466 Beare, M. H., Gregorich, E. G. and St-Georges, P.: Compaction effects on CO₂ and N₂O production during
467 drying and rewetting of soil, *Soil Biol. Biochem.*, 41(3), 611–621, doi:10.1016/j.soilbio.2008.12.024, 2009.
- 468 Bender, S. F., Plantenga, F., Neftel, A., Jocher, M., Oberholzer, H.-R., Köhl, L., Giles, M., Daniell, T. J. and van
469 der Heijden, M. G.: Symbiotic relationships between soil fungi and plants reduce N₂O emissions from soil,
470 *ISME J.*, 8(6), 1336–1345, doi:10.1038/ismej.2013.224, 2014.
- 471 Blom, C. W. P. M., Bögemann, G. M., Laan, P., van der Sman, A. J. M., van de Steeg, H. M. and Voesenek, L.
472 A. C. J.: Adaptations to flooding in plants from river areas, *Aquat. Bot.*, 38(1), 29–47, doi:10.1016/0304-
473 3770(90)90097-5, 1990.
- 474 Blum, J. M., Su, Q., Ma, Y., Valverde-Pérez, B., Domingo-Félez, C., Jensen, M. M. and Smets, B. F.: The pH
475 dependency of N-converting enzymatic processes, pathways and microbes: Effect on net N₂O production,
476 *Environ. Microbiol.*, doi:10.1111/1462-2920.14063, 2018.
- 477 Böttcher, J., Weymann, D., Well, R., Von Der Heide, C., Schwen, A., Flessa, H. and Duijnsveld, W. H. M.:
478 Emission of groundwater-derived nitrous oxide into the atmosphere: model simulations based on a 15N field
479 experiment, *Eur. J. Soil Sci.*, 62(2), 216–225, doi:10.1111/j.1365-2389.2010.01311.x, 2011.
- 480 Butterbach-Bahl, K., Baggs, E. M., Dannenmann, M., Kiese, R. and Zechmeister-Boltenstern, S.: Nitrous oxide
481 emissions from soils: how well do we understand the processes and their controls?, *Philos. Trans. R. Soc. Lond.*
482 *B. Biol. Sci.*, 368(1621), 20130122, doi:10.1098/rstb.2013.0122, 2013.
- 483 Ciais, P., Sabine, C., Bala, G., Bopp, L., Brovkin, V., Canadell, J., Chhabra, A., DeFries, R., Galloway, J.,
484 Heimann, M., Jones, C., Quéré, C. Le, Myneni, R. B., Piao, S. and Thornton, P.: Carbon and Other
485 Biogeochemical Cycles, in *Climate Change 2013 - The Physical Science Basis*, edited by Intergovernmental
486 Panel on Climate Change, pp. 465–570, Cambridge University Press, Cambridge., 2013.
- 487 Diba, F., Shimizu, M. and Hatano, R.: Effects of soil aggregate size, moisture content and fertilizer management
488 on nitrous oxide production in a volcanic ash soil, *Soil Sci. Plant Nutr.*, 57(5), 733–747,
489 doi:10.1080/00380768.2011.604767, 2011.
- 490 Drury, C. ., Yang, X. ., Reynolds, W. . and Tan, C. .: Influence of crop rotation and aggregate size on carbon
491 dioxide production and denitrification, *Soil Tillage Res.*, 79(1), 87–100, doi:10.1016/j.still.2004.03.020, 2004.
- 492 Ebrahimi, A. and Or, D.: Microbial community dynamics in soil aggregates shape biogeochemical gas fluxes
493 from soil profiles – upscaling an aggregate biophysical model, *Glob. Chang. Biol.*, 22(9), 3141–3156,
494 doi:10.1111/gcb.13345, 2016.
- 495 Elliott, A. E. T. and Coleman, D. C.: Oikos Editorial Office Let the Soil Work for Us Proceedings of the 4th
496 European Ecology Symposium 7-12 September 1986 , Wageningen Published by : Oikos Editorial Office Stable
497 URL : <http://www.jstor.org/stable/20112982> Let the soil work for us, *Ecol. Bull.*, (39), 22–32, 1988.
- 498 Fender, A.-C., Leuschner, C., Schützenmeister, K., Gansert, D. and Jungkunst, H. F.: Rhizosphere effects of tree



- 499 species – Large reduction of N₂O emission by saplings of ash, but not of beech, in temperate forest soil, *Eur. J.*
500 *Soil Biol.*, 54, 7–15, doi:10.1016/j.ejsobi.2012.10.010, 2013.
- 501 Forster, P., V. Ramaswamy, P. Artaxo, T. Berntsen, R. Betts, D.W. Fahey, J. Haywood, J. Lean, D.C. Lowe, G.
502 Myhre, J. Nganga, R. Prinn, G. Raga, M. S. and R. V. D.: Changes in Atmospheric Constituents and in Radiative
503 Forcing., 2007.
- 504 Frame, C. H., Lau, E., Joseph Nolan, E., Goepfert, T. J. and Lehmann, M. F.: Acidification enhances hybrid
505 N₂O production associated with aquatic ammonia-oxidizing microorganisms, *Front. Microbiol.*, 7(JAN), 1–23,
506 doi:10.3389/fmicb.2016.02104, 2017.
- 507 Gee, G. W. and Bauder, J. W.: Particle-size Analysis, in *Physical and Mineralogical Methods-Agronomy*
508 *Monograph no. 9*, edited by A. Klute, pp. 383–411, American Society of Agronomy-Soil Science Society of
509 America, Madison, WI., 1986.
- 510 Goldberg, S. D., Knorr, K. H., Blodau, C., Lischeid, G. and Gebauer, G.: Impact of altering the water table
511 height of an acidic fen on N₂O and NO fluxes and soil concentrations, *Glob. Chang. Biol.*, 16(1), 220–233,
512 doi:10.1111/j.1365-2486.2009.02015.x, 2010.
- 513 GraphPad Software Inc.: GraphPad Prism 7.04, La Jolla, CA, www.graphpad.com, 2017.
- 514 Groffman, P. M. and Tiedje, J. M.: Denitrification Hysteresis During Wetting and Drying Cycles in Soil, *Soil Sci.*
515 *Soc. Am. J.*, 52(6), 1626, doi:10.2136/sssaj1988.03615995005200060022x, 1988.
- 516 Hartmann, D. J., Klein Tank, A. M. G., Rusticucci, M., Alexander, L. V., Brönnimann, S., Charabi, Y. A.-R.,
517 Dentener, F. J., Dlugokencky, E. J., Easterling, D. R., Kaplan, A., Soden, B. J., Thorne, P. W., Wild, M. and
518 Zhai, P.: Observations: Atmosphere and Surface, in *Climate Change 2013 - The Physical Science Basis*, edited
519 by Intergovernmental Panel on Climate Change, pp. 159–254, Cambridge University Press, Cambridge., 2013.
- 520 Hefting, M., Clément, J.-C., Dowrick, D., Cosandey, A. C., Bernal, S., Cimpian, C., Tatur, A., Burt, T. P. and
521 Pinay, G.: Water table elevation controls on soil nitrogen cycling in riparian wetlands along a European climatic
522 gradient, *Biogeochemistry*, 67(1), 113–134, doi:10.1023/B:BIOG.0000015320.69868.33, 2004.
- 523 Heinicke, M. and Kaupenjohann, M.: Effects of soil solution on the dynamics of N₂O emissions: a review, *Nutr.*
524 *Cycl. Agroecosystems*, 55(2), 133–157, doi:10.1023/A:1009842011599, 1999.
- 525 Hill, A. R.: Buried organic-rich horizons: their role as nitrogen sources in stream riparian zones,
526 *Biogeochemistry*, 104(1–3), 347–363, doi:10.1007/s10533-010-9507-5, 2011.
- 527 Hu, H.-W., Macdonald, C. A., Trivedi, P., Holmes, B., Bodrossy, L., He, J.-Z. and Singh, B. K.: Water addition
528 regulates the metabolic activity of ammonia oxidizers responding to environmental perturbations in dry
529 subhumid ecosystems, *Environ. Microbiol.*, 17(2), 444–461, doi:10.1111/1462-2920.12481, 2015.
- 530 Jahangir, M. M. R., Roobroeck, D., Van Cleemput, O. and Boeckx, P.: Spatial variability and
531 biophysicochemical controls on N₂O emissions from differently tilled arable soils, *Biol. Fertil. Soils*, 47(7),
532 753–766, doi:10.1007/s00374-011-0580-2, 2011.
- 533 Jørgensen, C. J., Struwe, S. and Elberling, B.: Temporal trends in N₂O flux dynamics in a Danish wetland -
534 effects of plant-mediated gas transport of N₂O and O₂ following changes in water level and soil mineral-N
535 availability, *Glob. Chang. Biol.*, 18(1), 210–222, doi:10.1111/j.1365-2486.2011.02485.x, 2012.
- 536 Khalil, K., Renault, P. and Mary, B.: Effects of transient anaerobic conditions in the presence of acetylene on
537 subsequent aerobic respiration and N₂O emission by soil aggregates, *Soil Biol. Biochem.*, 37(7), 1333–1342,
538 doi:10.1016/j.soilbio.2004.11.029, 2005.
- 539 Koschorreck, M. and Darwich, A.: Nitrogen dynamics in seasonally flooded soils in the Amazon floodplain, *Wetl.*



- 540 Ecol. Manag., 11, 317–330, 1998.
- 541 Kowalik, P. J. and Randerson, P. F.: Nitrogen and phosphorus removal by willow stands irrigated with municipal
542 waste water? A review of the Polish experience, *Biomass and Bioenergy*, 6(1–2), 133–139, doi:10.1016/0961-
543 9534(94)90092-2, 1994.
- 544 Kuzyakov, Y. and Blagodatskaya, E.: Microbial hotspots and hot moments in soil: Concept & review, *Soil Biol.*
545 *Biochem.*, 83, 184–199, doi:10.1016/j.soilbio.2015.01.025, 2015.
- 546 Li, X., Sørensen, P., Olesen, J. E. and Petersen, S. O.: Evidence for denitrification as main source of N₂O
547 emission from residue-amended soil, *Soil Biol. Biochem.*, 92, 153–160, doi:10.1016/j.soilbio.2015.10.008, 2016.
- 548 Loecke, T. D. and Robertson, G. P.: Soil resource heterogeneity in terms of litter aggregation promotes nitrous
549 oxide fluxes and slows decomposition, *Soil Biol. Biochem.*, 41(2), 228–235, doi:10.1016/j.soilbio.2008.10.017,
550 2009.
- 551 Luster, J., Göttlein, A., Nowack, B. and Sarret, G.: Sampling, defining, characterising and modeling the
552 rhizosphere—the soil science tool box, *Plant Soil*, 321(1–2), 457–482, doi:10.1007/s11104-008-9781-3, 2009.
- 553 Manucharova, N. A., Stepanov, A. L. and Umarov, M. M.: Microbial transformation of nitrogen in water-stable
554 aggregates of various soil types, *EURASIAN SOIL Sci.*, 34(10), 1125–1131, 2001.
- 555 Morley, N., Baggs, E. M., Dörsch, P. and Bakken, L.: Production of NO, N₂O and N₂ by extracted soil bacteria,
556 regulation by NO₂- and O₂ concentrations, *FEMS Microbiol. Ecol.*, 65(1), 102–112, doi:10.1111/j.1574-
557 6941.2008.00495.x, 2008.
- 558 Myrold, D. D., Pett-Ridge, J. and Bottomley, P. J.: Nitrogen Mineralization and Assimilation at Millimeter
559 Scales, in *Methods in Enzymology*, vol. 496, pp. 91–114, Elsevier Inc., 2011.
- 560 Neira, J., Ortiz, M., Morales, L. and Acevedo, E.: Oxygen diffusion in soils: Understanding the factors and
561 processes needed for modeling, *Chil. J. Agric. Res.*, 75(August), 35–44, doi:10.4067/S0718-
562 58392015000300005, 2015.
- 563 Oades, J. M.: Soil organic matter and structural stability: mechanisms and implications for management, *Plant*
564 *Soil*, 76(1–3), 319–337, doi:10.1007/BF02205590, 1984.
- 565 Parkin, T. B.: Soil Microsites as a Source of Denitrification Variability, *Soil Sci. Soc. Am. J.*, 51, 1194–1199,
566 1987.
- 567 Philippot, L., Hallin, S., Börjesson, G. and Baggs, E. M.: Biochemical cycling in the rhizosphere having an
568 impact on global change, *Plant Soil*, 321(1–2), 61–81, doi:10.1007/s11104-008-9796-9, 2009.
- 569 R Core Team: R: A Language and Environment for Statistical Computing, R Found. Stat. Comput., Vienna,
570 <https://www.R-project.org/>, 2018.
- 571 Rabot, E., Hénault, C. and Cousin, I.: Temporal Variability of Nitrous Oxide Emissions by Soils as Affected by
572 Hydric History, *Soil Sci. Soc. Am. J.*, 78(2), 434, doi:10.2136/sssaj2013.07.0311, 2014.
- 573 Randerson, P. F., Moran, C. and Bialowiec, A.: Oxygen transfer capacity of willow (*Salix viminalis* L.),
574 *Biomass and Bioenergy*, 35(5), 2306–2309, doi:10.1016/j.biombioe.2011.02.018, 2011.
- 575 Ravishankara, A. R., Daniel, J. S. and Portmann, R. W.: Nitrous Oxide (N₂O): The Dominant Ozone-Depleting
576 Substance Emitted in the 21st Century, *Science* (80-.), 326(5949), 123–125, doi:10.1126/science.1176985,
577 2009.
- 578 Renault, P. and Stengel, P.: Modeling Oxygen Diffusion in Aggregated Soils: I. Anaerobiosis inside the
579 Aggregates, *Soil Sci. Soc. Am. J.*, 58(4), 1017, doi:10.2136/sssaj1994.03615995005800040004x, 1994.
- 580 Robertson, G. P. and Groffman, P. M.: Nitrogen Transformations, in *Soil Microbiology, Ecology and*



- 581 Biochemistry, pp. 421–446, Elsevier., 2015.
- 582 Ruser, R., Flessa, H., Russow, R., Schmidt, G., Buegger, F. and Munch, J. C.: Emission of N₂O, N₂ and CO₂
583 from soil fertilized with nitrate: Effect of compaction, soil moisture and rewetting, *Soil Biol. Biochem.*, 38(2),
584 263–274, doi:10.1016/j.soilbio.2005.05.005, 2006.
- 585 Samaritani, E., Shrestha, J., Fournier, B., Frossard, E., Gillet, F., Guenat, C., Niklaus, P. A., Pasquale, N.,
586 Tockner, K., Mitchell, E. A. D. and Luster, J.: Heterogeneity of soil carbon pools and fluxes in a channelized and
587 a restored floodplain section (Thur River, Switzerland), *Hydrol. Earth Syst. Sci.*, 15(6), 1757–1769,
588 doi:10.5194/hess-15-1757-2011, 2011.
- 589 Sey, B. K., Manceur, A. M., Whalen, J. K., Gregorich, E. G. and Rochette, P.: Small-scale heterogeneity in
590 carbon dioxide, nitrous oxide and methane production from aggregates of a cultivated sandy-loam soil, *Soil Biol.*
591 *Biochem.*, 40(9), 2468–2473, doi:10.1016/j.soilbio.2008.05.012, 2008.
- 592 Shrestha, J., Niklaus, P. a, Frossard, E., Samaritani, E., Huber, B., Barnard, R. L., Schleppi, P., Tockner, K. and
593 Luster, J.: Soil nitrogen dynamics in a river floodplain mosaic., *J. Environ. Qual.*, 41(6), 2033–45,
594 doi:10.2134/jeq2012.0059, 2012.
- 595 Six, J., Bossuyt, H., Degryze, S. and Denef, K.: A history of research on the link between (micro)aggregates, soil
596 biota, and soil organic matter dynamics, *Soil Tillage Res.*, 79(1), 7–31, doi:10.1016/j.still.2004.03.008, 2004.
- 597 Spott, O., Russow, R. and Stange, C. F.: Formation of hybrid N₂O and hybrid N₂ due to codenitrification: First
598 review of a barely considered process of microbially mediated N-nitrosation, *Soil Biol. Biochem.*, 43(10), 1995–
599 2011, doi:10.1016/j.soilbio.2011.06.014, 2011.
- 600 Stolk, P. C., Hendriks, R. F. A., Jacobs, C. M. J., Moors, E. J. and Kabat, P.: Modelling the effect of aggregates
601 on N₂O emission from denitrification in an agricultural peat soil, *Biogeosciences*, 8(9), 2649–2663,
602 doi:10.5194/bg-8-2649-2011, 2011.
- 603 Thorbjørn, A., Moldrup, P., Blendstrup, H., Komatsu, T. and Rolston, D. E.: A Gas Diffusivity Model Based on
604 Air-, Solid-, and Water-Phase Resistance in Variably Saturated Soil, *Vadose Zo. J.*, 7(4), 1276,
605 doi:10.2136/vzj2008.0023, 2008.
- 606 Tisdall, J. M. and Oades, J. M.: Organic matter and water-stable aggregates in soils, *J. Soil Sci.*, 33(2), 141–163,
607 doi:10.1111/j.1365-2389.1982.tb01755.x, 1982.
- 608 Totsche, K. U., Amelung, W., Gerzabek, M. H., Guggenberger, G., Klumpp, E., Knief, C., Lehdorff, E.,
609 Mikutta, R., Peth, S., Prechtel, A., Ray, N. and Kögel-Knabner, I.: Microaggregates in soils, *J. Plant Nutr. Soil*
610 *Sci.*, 1–33, doi:10.1002/jpln.201600451, 2017.
- 611 Vieten, B., Conen, F., Neftel, A. and Alewell, C.: Respiration of nitrous oxide in suboxic soil, *Eur. J. Soil Sci.*,
612 60(3), 332–337, doi:10.1111/j.1365-2389.2009.01125.x, 2009.
- 613 Walthert, L., Graf, U., Kammer, A., Luster, J., Pezzotta, D., Zimmermann, S. and Hagedorn, F.: Determination
614 of organic and inorganic carbon, $\delta^{13}\text{C}$, and nitrogen in soils containing carbonates after acid fumigation with
615 HCl, *J. Plant Nutr. Soil Sci.*, 173(2), 207–216, doi:10.1002/jpln.200900158, 2010.
- 616 Young, I. . and Ritz, K.: Tillage, habitat space and function of soil microbes, *Soil Tillage Res.*, 53(3–4), 201–213,
617 doi:10.1016/S0167-1987(99)00106-3, 2000.
- 618 Zhu, X., Burger, M., Doane, T. a and Horwath, W. R.: Ammonia oxidation pathways and nitrifier denitrification
619 are significant sources of N₂O and NO under low oxygen availability, *Pnas*, 110(16), 6328–6333,
620 doi:10.1073/pnas.1219993110/-/DCSupplemental.www.pnas.org/cgi/doi/10.1073/pnas.1219993110, 2013.
- 621



622 **Table 1: Physicochemical properties of the two aggregate size fractions (macroaggregates and microaggregates) and**
 623 **added leaf litter. C_{org} and N_{tot} of the aggregates was measured in triplicates. The leaf litter was analyzed in four**
 624 **replicates. Final pH and texture of model soil 1 and 2 was measured in duplicates (means \pm SD)**

		Macroaggregates	Microaggregates	Litter (<i>Salix v. L.</i>)
C_{org}	g kg ⁻¹	19.22 \pm 0.55	21.56 \pm 2.39	459.9 \pm 2.55
Total N	g kg ⁻¹	1.58 \pm 0.02	1.35 \pm 0.14	27.39 \pm 0.15
C:N ratio		12.16 \pm 0.22	15.99 \pm 0.71	16.79 \pm 0.06
		Model soil 1	Model soil 2	
pH (CaCl ₂)		8 \pm 0.02	7.56 \pm 0.01	
sand	%	71.25 \pm 0.05	70.7 \pm 0.50	
silt	%	20 \pm 0.30	21.1 \pm 0.60	
clay	%	8.75 \pm 0.25	8.2 \pm 0.10	

625

626 **Table 2: Overview of treatments in the flooding–drying experiment**

	LAU	SAU	LAL	SAL	LAP	SAP
Model Soil 1 (LA)	+	-	+	-	+	-
Model Soil 2 (SA)	-	+	-	+	-	+
Leaf litter (<i>Salix v.</i>)	-	-	+	+	-	-
<i>Salix v.</i>	-	-	-	-	+	+

627



628 **Figure Captions**

629 **Figure 1:** Schematic of a mesocosm with gas sampling valves (1), Ag/AgCl reference electrode (2), Pt redox electrodes
630 (3), suction cups (4), volumetric water content sensors (5), vent (6), and water inlet/outlet (7). The top part is only
631 attached during gas sampling.

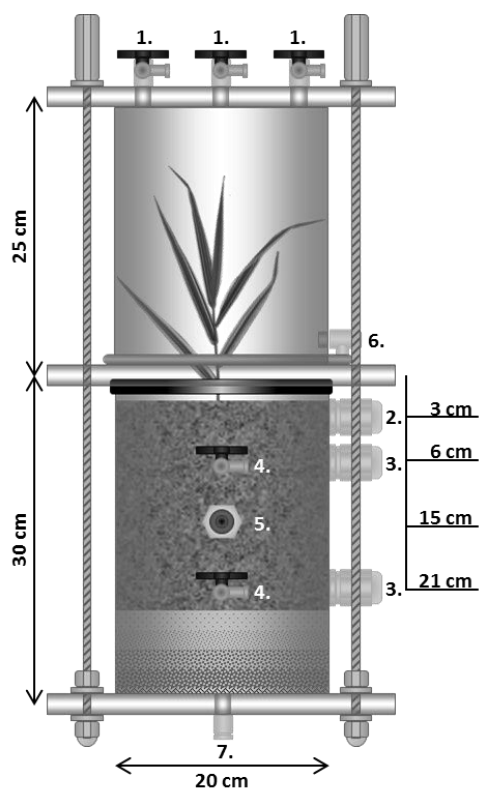
632 **Figure 2:** Mean N₂O emission during the flooding–drying experiment from large-aggregate model soil (LA; filled
633 circles) and small-aggregate model soil (SA, open circles), and corresponding water-filled pore space (WFPS) in LA
634 (filled triangles) and SA (open triangles). Unamended soils (A), litter addition (B) and plant treatment (C). Flooding
635 phase indicated by the grey area. Symbols indicate means; error bars are SE; n= 6.

636 **Figure 3:** Redox potential relative to standard hydrogen electrode during the flooding–drying experiment in 5 cm and
637 20 cm depth (mean ± SE; n=6). Unamended soils (a and d, respectively), litter addition (b and e, respectively), plant
638 treatment (c and f, respectively). LA (filled circles) and SA (open circles); the dotted line at 250 mV marks the
639 threshold, below which denitrification is expected to occur.

640 **Figure 4:** DOC (circles), nitrate (squares), nitrite (diamonds) and ammonium (triangles) concentrations in pore water
641 during the flooding–drying experiment. LA (filled symbols) and SA (empty symbols). Unamended soils (a, d, g and j,
642 respectively), litter addition (b, e, h and k, respectively) and plant treatment (c, f, j and l, respectively).; (mean ± SE;
643 n=6).

644 **Figure 5:** Integrated N₂O fluxes over the 14 days period of elevated N₂O emissions in the drying phase of the flooding–
645 drying experiment (mean ± SE; n= 6). Black bars represent model soil 1 (macroaggregates 250-4000µm) whereas
646 model soil 2 (microaggregates < 250µm) is depicted as white bars. Significant differences among the six treatments are
647 denoted by different lower case letters at adj. P < 0.05.

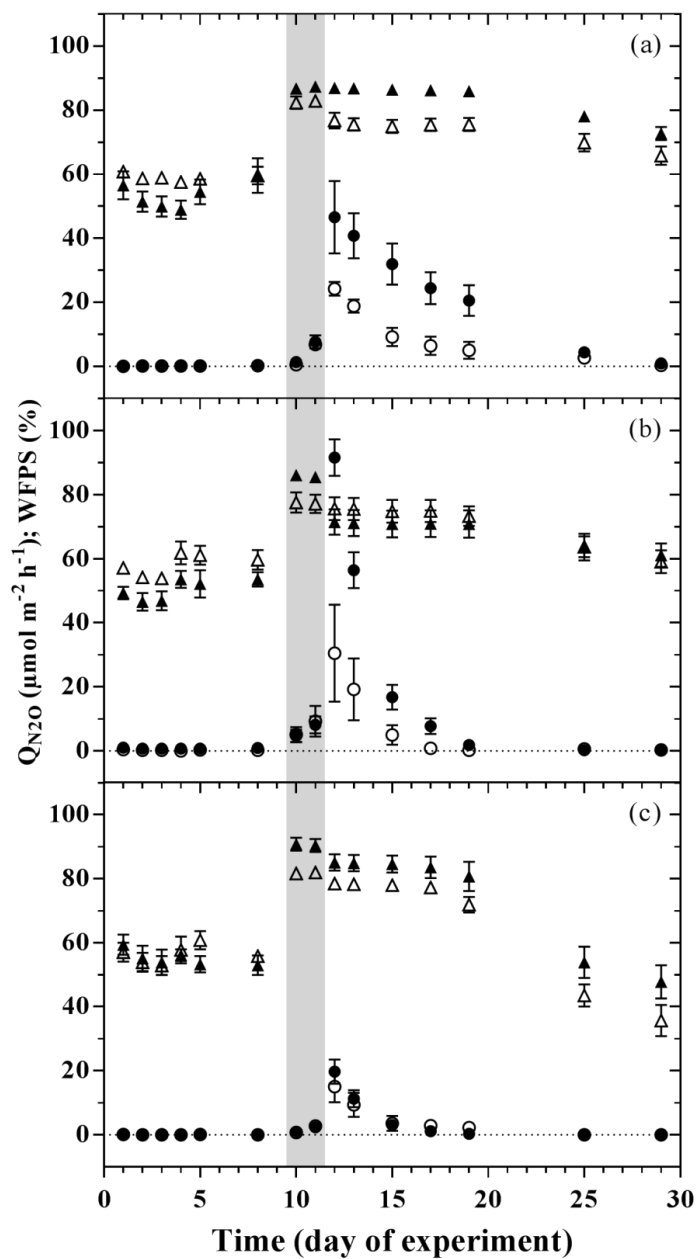
648



649

650 Figure 1

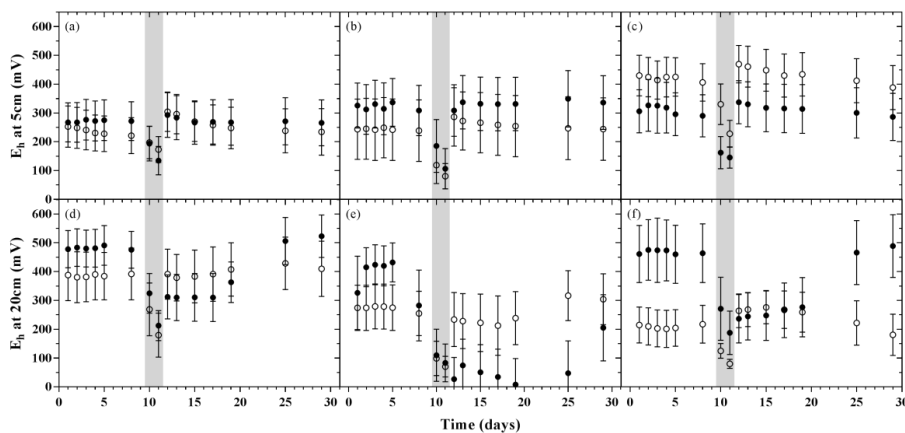
651



652

653 Figure 2

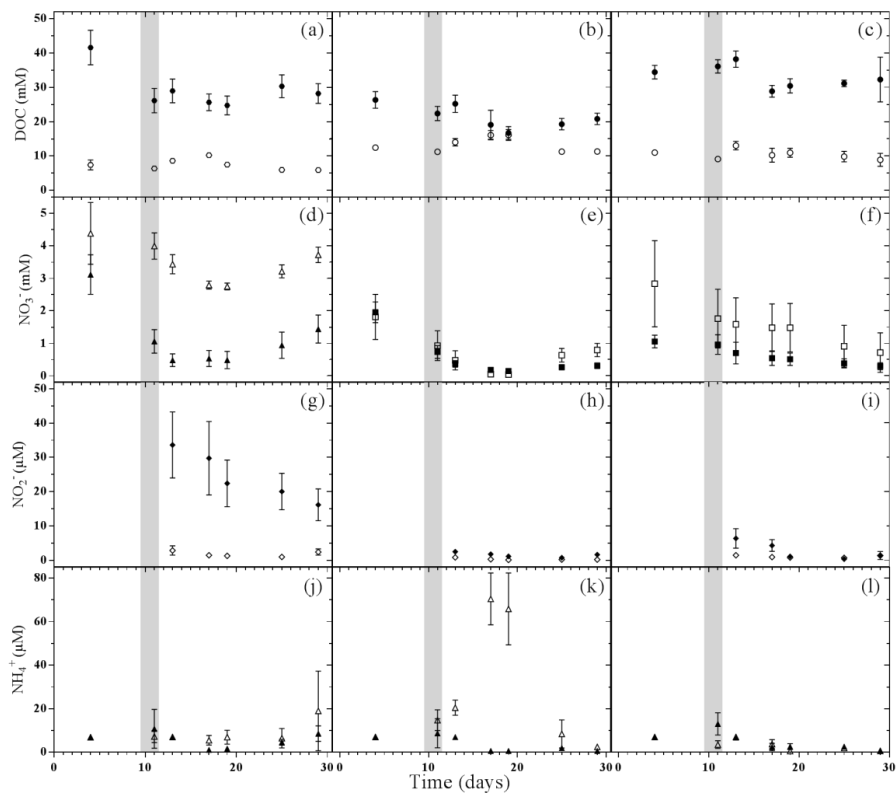
654



655

656 Figure 3

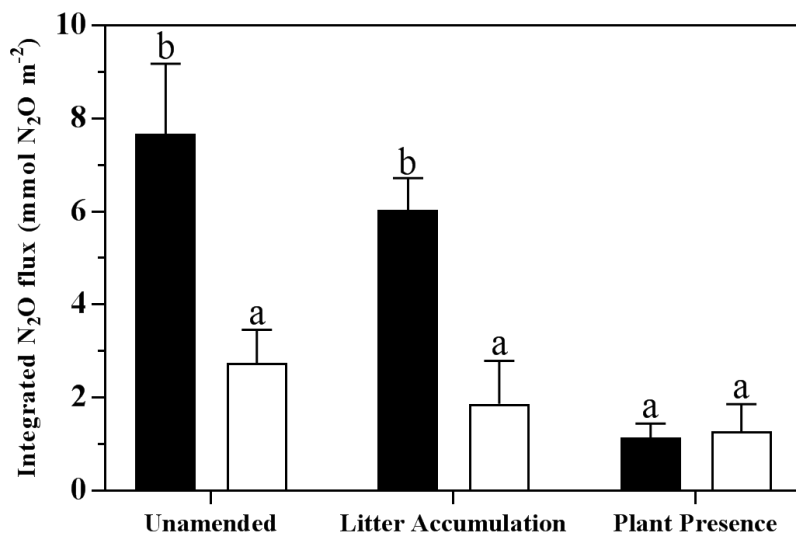
657



658

659 Figure 4

660



661

662 Figure 5